Tectonophysics 472 (2009) 323–339

Contents lists available at ScienceDirect

Tectonophysics

journal homepage: www.elsevier.com/locate/tecto

A three-dimensional model of the Early Precambrian crust under the southeastern Fennoscandian Shield: Karelia craton and Belomorian tectonic province

M. Mints [a,*], A. Suleimanov [b], N. Zamozhniaya [b], V. Stupak [b]

[a] *Geological Institute of the Russian Academy of Sciences, Pyzhevsky 7, 119117 Moscow, Russia*
[b] *Spetsgeophysica, 107140 Moscow Region, Russia*

ARTICLE INFO

Article history:
Received 23 May 2007
Received in revised form 10 October 2008
Accepted 1 December 2008
Available online 13 December 2008

Keywords:
Reflection seismics
Fennoscandian Shield
Karelia craton
Belomorian province
Deep crustal structure
3-D modeling of the crustal structure

ABSTRACT

The Early Precambrian structures of the Archaean Karelia craton and Belomorian tectonic province have been investigated by reflection seismology. Integration of the existing geological database for these two entities and adjacent tectonic units with the seismic data for the crust and upper mantle along the 1-EU geotraverse and cross-traverse 4B totaling c.1300 km allows development of a three-dimensional model of the deep structure of the southeastern Fennoscandian Shield. Interpretation of the seismic data provides evidence that the Early Precambrian crust is characterized by inclined layering. The crustal architecture is a combination of thrust–nappe and thrust–underthrust structural assemblages consisting of Neoarchaean and Palaeoproterozoic rocks that were subsequently further deformed during uplift and emplacement of granite-gneiss domes. The new model substantially modifies previous conceptions of this part of the shield as being constituted of blocks with sub-vertical margins and individual internal layering. It is apparent that the surface traces of gently dipping boundaries are defined by the erosion level and consequently these boundaries are not those of particular “tectonic blocks” in the traditional sense.

1. Introduction

In 1995, a major Russian project was begun to study the deep structure of the Earth's crust and upper mantle in the eastern Fennoscandian Shield by the CMP (common midpoint, or common depth point — CDP) method based on recording near-vertical seismic reflections. As part of a program of deep investigations of the Earth's crust and upper mantle of the Russian Ministry of the Natural Resources, the geophysical enterprise “Spetsgeofizika” undertook surveys along the 1-EU geotraverse and cross-traverse 4B. Investigations along line 4B also contributed to the SVEKALAPKO project of the international EUROPROBE Program. This paper is devoted to the main geological results of this study as they relate to the Early Precambrian structures of the Archaean Karelia craton and Belomorian tectonic province and their mutual structural and evolutionary relationships as well as the relationships with the adjacent tectonic units: Archaean Kola craton, the Palaeoproterozoic Svecofennian accretionary orogen and intracratonic Palaeoproterozoic volcano-sedimentary belts.

High-resolution seismic images obtained by the CMP technology reveal a significantly more complex and different structures of the Earth's crust than had previously been assumed. They show that gently dipping and relatively steep boundaries as well as other features of diverse form can be observed everywhere within the crust. It is important to note that many seismic boundaries in CMP sections reach the Earth's surface, in contrast to those in DSS (deep seismic sounding) sections. It was established that the crust–mantle discontinuity is in most cases of complex character.

Integration of the existing geological maps and available geological (in the widest sense: structural, geochemical, geochronological and other) data with results of geological interpretation of seismic images of the crust and upper mantle along the 1-EU geotraverse and cross-traverse 4B – totaling a length of some 1300 km – leads to a three-dimensional model of the deep structure of the study area and a significant revision of previous ideas on the deep structure and Early Precambrian evolution of eastern Fennoscandia.

2. Geological background

The Archaean Karelia craton and Belomorian tectonic province are the main tectonic units within the studied area in the eastern part of the Fennoscandian Shield (Figs. 1 and 2). The Archaean Kola craton is situated to the northeast from the Belomorian province. Volcano-sedimentary and volcano-plutonic assemblages of the Palaeoproterozoic Svecofennian accretionary orogen border the Karelia craton on the south and southwest.

Available geological data permit us to distinguish a number of granite-greenstone terrains within the Karelia craton (see Glebovitsky, 2005; Slabunov et al., 2006 and references therein). The Vodla and Iisalmi granite-greenstone terrains contain the most ancient rocks: granitoids and gneisses of c.3.14–2.62 Ga and greenstone belts

* Corresponding author.
E-mail address: mints@ginras.ru (M. Mints).

0040-1951/$ – see front matter © 2008 Published by Elsevier B.V.
doi:10.1016/j.tecto.2008.12.008

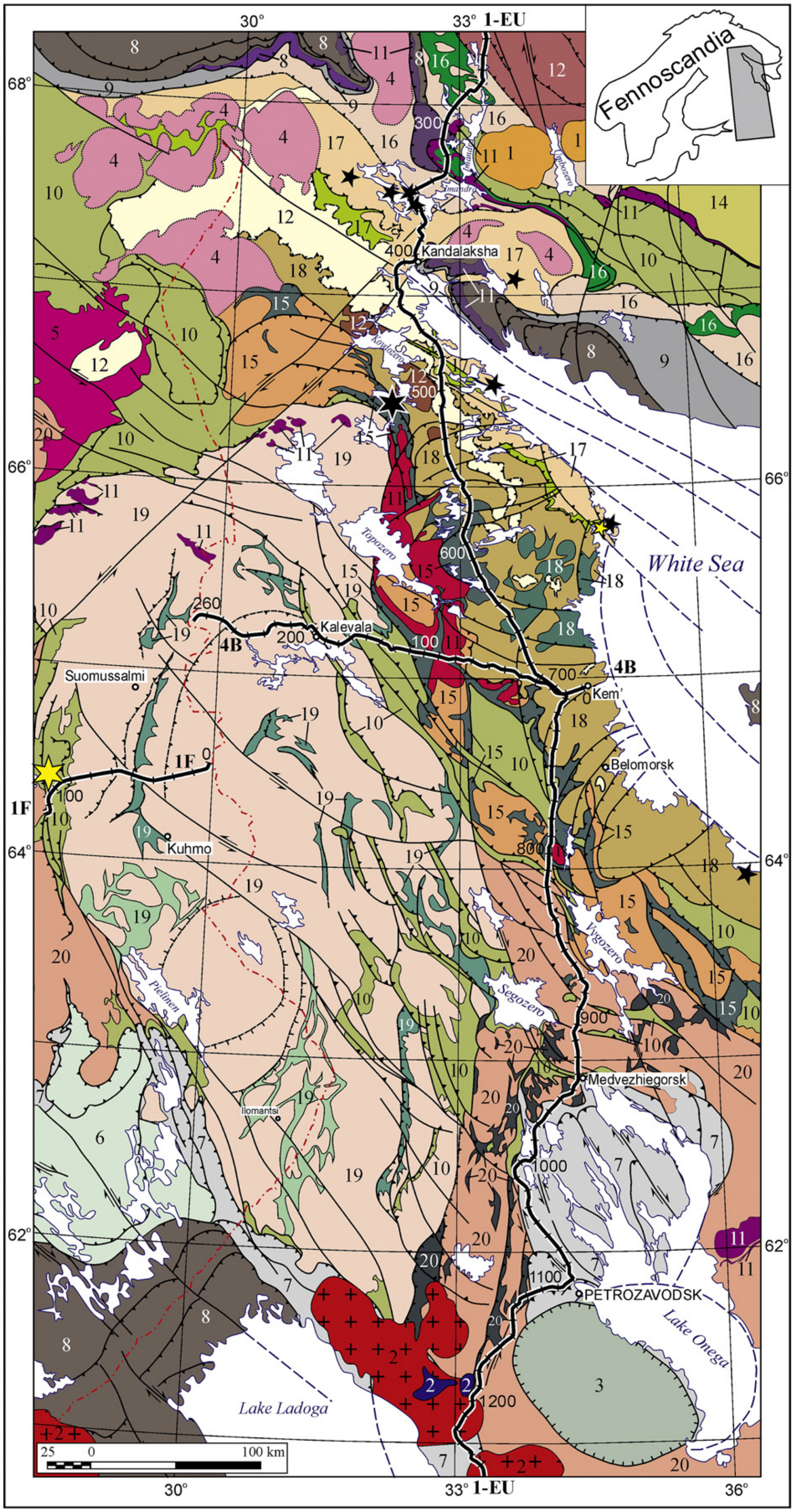

Fig. 1. Geological map of the southeastern Fennoscandian Shield. The map was compiled by M. Mints on a basis of integration of the existing geological maps and available geological (in the wide sense: structural, geochemical, geochronological and other) data with results of geological interpretation of seismic images of the crust; the Geological map of the Fennoscandian Shield in scale 1:2 000 000 (Koistinen et al., 2001) was used as a starting-point. Legend includes signs for middle and low crustal units shown at Figs. 5–7. (For interpretation of the references to color in this figure legend, the reader is referred to the web version of this article.)

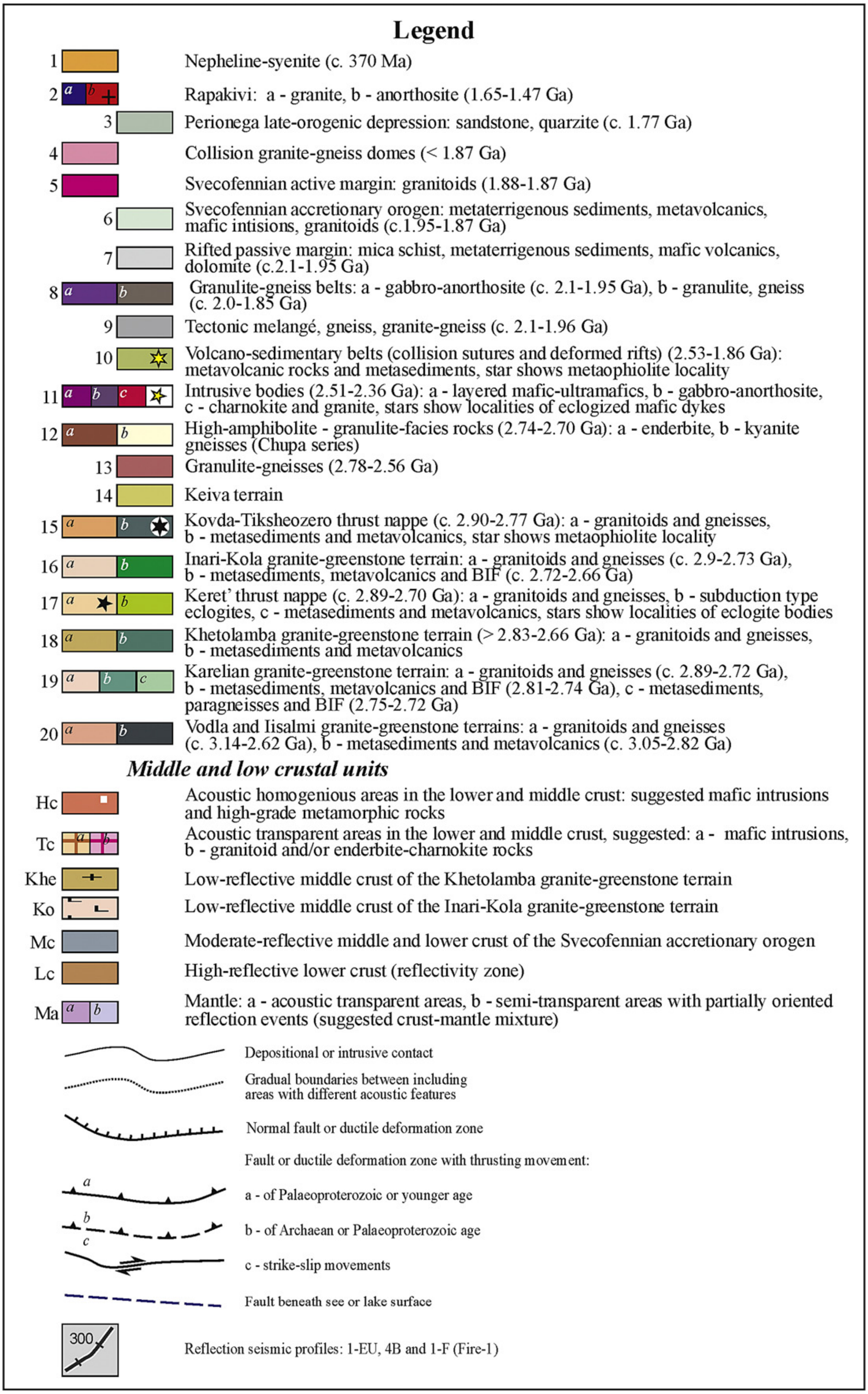

Fig. 1 (*continued*).

formed by the c.3.05–2.82 Ga volcano-sedimentary assemblages. Tonalite–tronjemite–granodiorite (TTG) granitoids and gneisses of 2.89–2.72 Ga dominate within the Karelian granite-greenstone terrain. Karelian greenstone belts are built by metasediments, mafic, komatiitic and intermediate-felsic metavolcanics and BIF dated at 2.81–2.74 Ga. Younger paragneiss belts (2.75–2.72 Ga) consist mainly

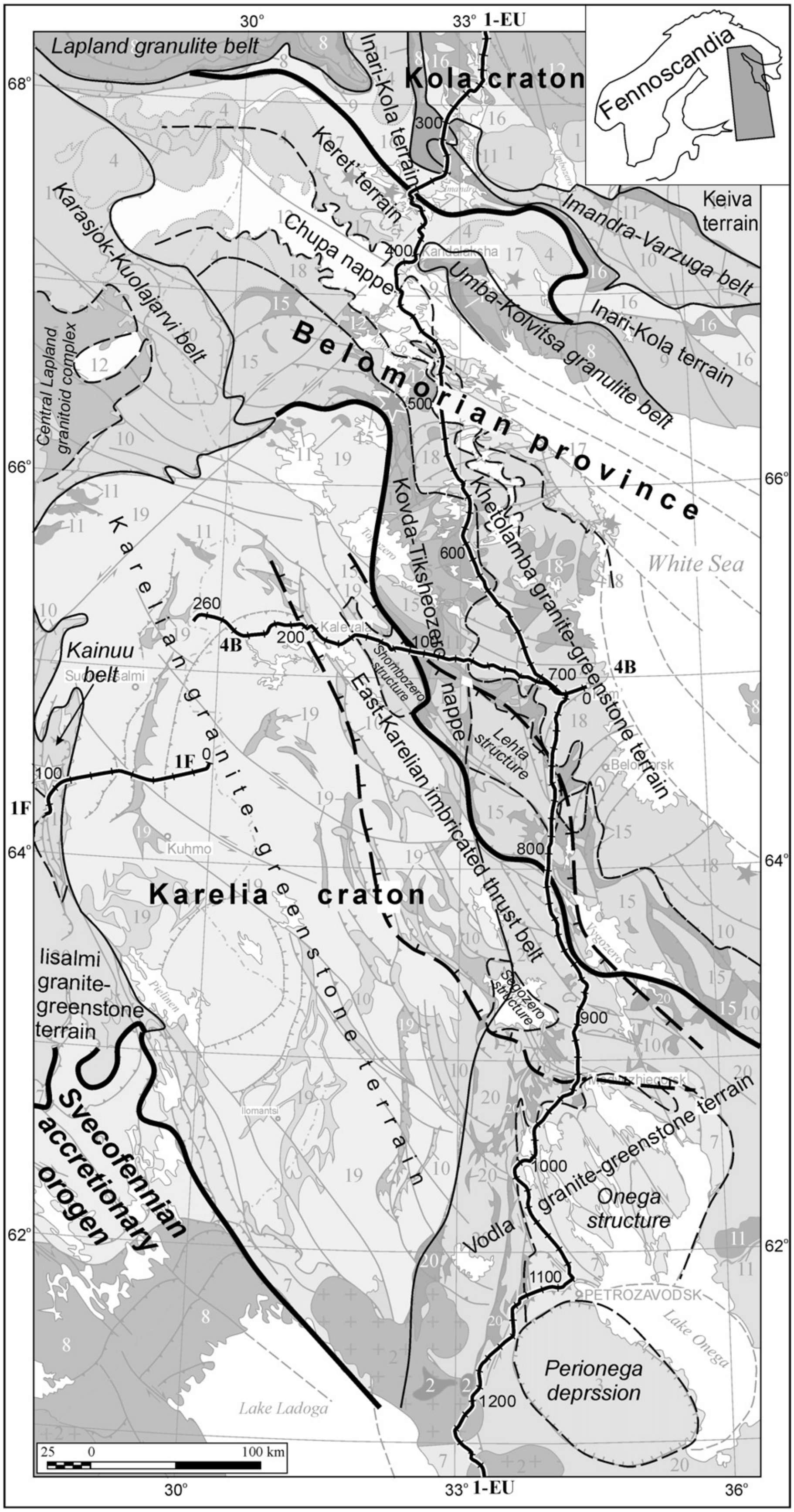

Fig. 2. Main tectonic units in the southeastern Fennoscandian Shield (translucent background is based on the monochrome of Fig. 1). Boundaries between main tectonic units are shown as bold lines, boundaries of granite-greenstone terrains within Karelia craton, of tectonic units within Belomorian province and contours of the Palaeoproterozoic belts are shown as solid thin lines and as thin broken lines across Palaeoproterozoic domes; the Palaeoproterozoic East-Karelian imbricate thrust belt is picked out roughly by bold broken lines.

of metasediments, paragneisses and banded iron formation (BIF). Postcollision granitoids of sanukitoid type (2.74–2.72 Ga) are less widespread (not shown in Fig. 1).

The Inari–Kola granite-greenstone terrain is situated to the north largely beyond the limits of the study area. However the crustal boundary between this terrain and the Belomorian province is an important topic of this paper. Granite-gneiss complexes (mainly TTG-gneisses) were formed between c.2.9 and 2.73 Ga, poorly dated metasediments, metavolcanics and BIF assemblages of greenstone belts within the Inari–Kola terrain fall in the 2.72–2.66 Ga interval.

The Belomorian tectonic province has during the long period of time been of special interest to geologists (e.g., Shchiptsov, 2005; Slabunov et al., 2006 and references therein). The province is distinguished by intensely repeated deformation and high- and moderate-pressure metamorphism that occurred in both the Neoarchaean and Palaeoproterozoic. The Khetolamba granite-greenstone terrain (>2.83–2.66 Ga) forms the main constituent of the Belomorian province (Miller et al., 2005). The Kovda–Tiksheozero thrust nappe separates the Khetolamba terrain and Karelia craton at the present-day surface. It is formed by TTG-granitoids and gneisses hosting metasediments and metavolcanics of several greenstone belts that were originated from c.2.90 to 2.77 Ga.

In turn, the Keret' tectonic nappe emplaced at the present-day surface between Khetolamba and Inari–Kola terrains contains c.2.89–2.70 Ga TTG-gneisses and greenstones. Chain of subduction type eclogite bodies has recently been discovered within Keret' gneisses. According to available data they belong at least to two generations, c.2.86 Ga and c.2.70 Ga (Volodichev et al., 2004; Konilov et al., 2005; Shchipansky et al., 2006). The Central Belomorian greenstone belt separating Keret' and Khetolamba terrains is formed by the mafic–ultramafic sequence that is no younger then 2.85 Ga. The available geological, isotopic, and geochemical data allow us to regard the mafic–ultramafic rocks of the greenstone complex as a tectonically disintegrated and metamorphosed fragment of the Mesoarchean ophiolitic association (Slabunov et al., 2006). A deep structure of the area that is discussed below together with above mentioned data (eclogite occurrences including) permit us to interpret this belt as the Mesoarchean suture zone (see Figs. 6 and 7 for location).

The synformal thrust nappe formed by upper-amphibolite- to granulite-facies kyanite gneisses (Chupa series) occupies the axial area of the Belomorian province. The rocks contain 3.11–2.96 Ga detrital zircon grains (Bibikova et al., 2004). Another zircon population dated at 2.83–2.79 Ga was interpreted as indicative of an early metamorphism but petrological evidence of that metamorphism remains equivocal. An inherited (detrital) nature of this population seems to us to be more realistic (see also Evins et al., 2002). High-pressure (up to 10–12 kbar) amphibolite-granulite facies metamorphism occurred 2.71–2.70 Ga ago (Bibikova et al., 2004).

Bibikova, Slabunov and co-workers suggested that the Belomorian province is a long-lived "mobile" belt created along the eastern margin of the Karelia craton as a result of a succession of events: westward (in present-day coordinates) subduction of the Archaean oceanic lithosphere beneath the Karelia craton, accretion of the island-arc complexes to the Karelia margin and final collision at approximately 2.75–2.65 Ga (Bibikova et al., 1999; Slabunov, 2005; Slabunov et al., 2006). Kyanite gneisses of the Chupa series were interpreted as a remnant of the accretionary prism. However, as evident from what follows, this model conflicts with reflection seismic images of the Belomorian crust.

Early Palaeoproterozoic layered mafic–ultramafic bodies intruded the upper crust of the Karelia craton 2.45–2.44 Ga ago (Hanski et al., 2001). Similar intrusions in the Kola craton were emplaced along the northern boundary of and within the Pechenga–Imandra–Varzuga belt at 2.51–2.40 Ga (Bayanova, 2004) (Pechenga structure at the northwestern flank of the Pechenga–Imandra–Varzuga belt is situated beyond the frame of the Figs. 1 and 2). Small intrusive bodies and dykes of gabbro-norite and lherzolite composition are dispersed within the Belomorian crust. Some of them underwent eclogite-facies metamorphism immediately after intrusion attesting to the great thickness of this crustal section to that time (c.2.45–2.42 Ga or younger) (Volodichev et al., 2004; Dokukina et al., 2006). At the same time (2.47–2.45 Ga) gabbro-anorthosite bodies intruded into the lower crust and underwent granulite-facies metamorphism (Mints et al., 2007 and references therein). At present these bodies are emplaced at the base of the Lapland granulite belt. Mafic magmatism was accompanied by intrusion of charnockites and granites and eruptions of quartz porphyries (ash-flows) at 2.45–2.36 Ga (Tugarinov and Bibikova, 1980; Levchenkov et al., 1994; Zlobin et al., 2005).

Like the Karelia craton, the Belomorian tectonic province is suggested to be a segment of the fragmented Neoarchaean supercontinent crossed and bounded by the Palaeoproterozoic sedimentary-volcanic belts, which can be interpreted as deformed rifts and, locally, as sutures: Pechenga–Imandra–Varzuga, North- and East-Karelian and Karasjok–Kuolajarvi belts. It is usually assumed that the Palaeoproterozoic sedimentary-volcanic «proto-cover» that occurred preserved within the limits of rift structures blanketed the Karelia granite-greenstone craton during the Palaeoproterozoic (e.g., Glebovitsky, 2005, and multiple references therein). These volcano-sedimentary successions with a predominance of mafic volcanics were formed at 2.50–2.43 Ga in Karelia (Hanski et al., 2001; Glebovitsky, 2005 and references therein) and c.2.45 to c.1.77 Ga ago in the Pechenga–Imandra–Varzuga belt (mainly Rb–Sr data (Balashov, 1996)). The general north-north-west strike of the Palaeoproterozoic belts within Karelia craton forms an acute angle with respect to the dominant north–south strike of the Neoarchaean greenstone belts. Among the Palaeoproterozoic belts, as a first approximation, two types of synclinal structures can be distinguished: (1) brachyform structures a few tens of kilometers to 300 km wide (the Shombozero, Lehta, Segozero and onega structures), and (2) narrow linear structures up to 200 km long and 2–10 km wide. For the first type, a gentle dip is characteristic. For the second type, a 60–80° dip is typical; vertical dips and overturning are common. Frequent absence of one of the limbs transforms them into monoclines (Sokolov, 1987).

For a long time crustal structure of the eastern Fennoscandian Shield was envisaged as a combination of "blocks" of crustal dimensions characterized by individual subhorizontal layering (e.g., Sharov, 1997; Korsman et al., 1999). Recently, however, a new understanding of the crustal architecture based on new geological, geochemical and deep seismic data has gained ground. Early Precambrian crust of the region appears to be an ensemble built by inclined crustal sheets and slices (Sharov, 2004; Mints et al., 2004a, b; Korja and Heikkinen, 2005; Kukkonen and Lahtinen, 2006) conforming to plate tectonic theory.

3. Characteristics of the field seismic experiment and data processing

The main parameters of the field seismic experiment are presented in Table 1. Source and recording parameters ensuring effective vibroseis operation and noise suppression in the geoseismic regime

Table 1
The main parameters of the field seismic experiment.

	Line 4B	Line 1-EU
	Specifications	
Recording	I/O-2+SN-388 200-channel	I/O-2 500-channel
Record length, s	25	25
Acquisition geometry	End-on	Symmetric split spread
Spread length, m	10,000	18,000
Receiver spacing, m	50	50
Shot interval, m	100	100
Geophone type	GS-20DX	GS-20DX
Vibrator type	SV-10-180	SV-20-150
Frequency limits, Hz	12–60	12–60
Sweep length, s	20	20
Vertical summing	8	8

of the eastern part of the Fennoscandian Shield were determined as a result of field tests. Features of the wavefield have been defined on the basis of both surface and deep seismic and geological conditions. Typical recorded seismogram is presented in Fig. 3. The wavefield obtained is extremely varied both in form and in amplitude attributes. The following should be attributed to the wavefield features: a limited extent of the strongest P-wave events and their interference nature. Spectral analysis of correlated seismograms made within different time intervals shows that, with selected source parameters, no sharp absorption of high-frequency components is observed and the dominant frequency of the recorded spectrum decreases slightly with depth and resides within the band of sweep generated (Fig. 3). Correlation harmonics do not exceed 10–15 dB.

The seismic data were processed using (1) standard dynamic and kinematic technology and (2) the method of differential seismics (MDS). Physico-mathematical aspects of MDS are discussed by Vasil'ev and Urupov (1978), Dyadyura (1992) and Stupak (2000). The program-and-methodology system of MDS involves the most effective elements of the controlled directional reception (CDR) procedure and the CMP method. MDS provides an analysis of the kinematic and dynamic parameters of seismic waves. It is based on a reciprocal point technique that provides a full and unequivocal solution of the inverse 2D seismic problem at any morphology of reflection boundaries. Processing begins with the parametric differential representation of seismic records. The main mathematical procedure is velocity sweeping that means the reflection directional stacking within a small summation window of the order of 5–11 channels of initial records. For each event detected in the process of stacking a set of parameters is defined: reflection time, time shift (dip), amplitude, frequency, and velocity. Thus, the wave form of the oscillating process is replaced by its parametric description. This reduces the volume of initial information substantially. Each travel-time curve portion represented parametrically is visualized as a vector consisted of ten parameters. Parametric representation is carried out under specified boundary conditions, which are defined by the properties of the geological environment (for instance, velocity no more than 8000 m/s, frequency within the range of a radiator, a ban on multiples and so on). A set of vectors, which fall into the same base, is written as standard seismic trace. After seismic record transformation, an interactive editing of seismic data is conducted for the purpose of rejecting the components, which do not bear the geologic information.

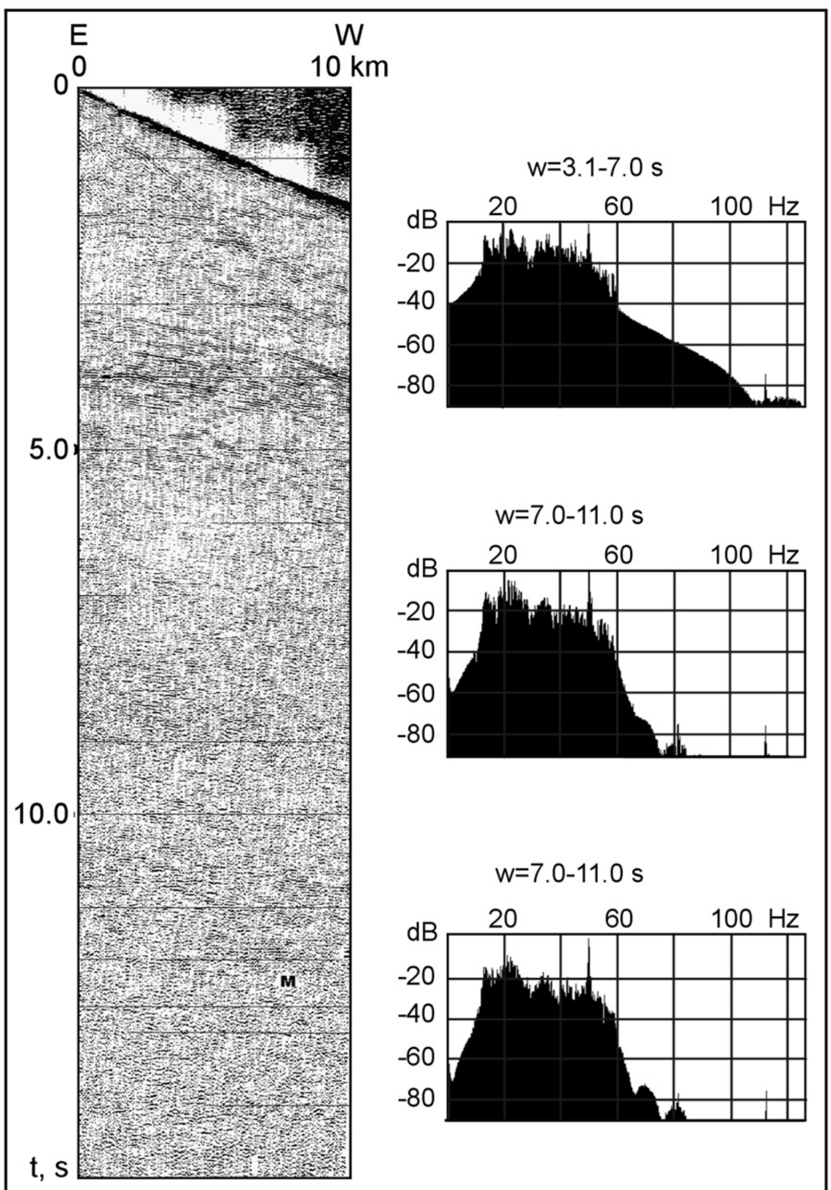

Fig. 3. Correlated seismogram and frequency spectrum, line 4B, stake 38.5. M — approximate position of diffuse Moho discontinuity.

MDS allows the calculation of the effective velocities, location, distribution and dip angles of reflecting elements. At the accepted dimension of depicted events as 400 m, the method made it possible to obtain detailed characteristics of the upper and middle portions of the Earth's crust down to 16–18 km depth. Individual seismic reflections from relatively "smooth" extended surfaces are overlapped and form continuous lines (boundaries). The MDS system gives also an opportunity to analyze traveltime and amplitude attributes (parameters) of seismic waves. This, in its turn, makes it possible to proceed to estimation of subsurface petrophysical properties.

Amplitudes of reflected waves (A) are correlated with the acoustic impedance (α) of contacting rock units. The relationship $A = f(\alpha)$ is not defined in quantitative terms, however, MDS allows the obtaining of the distribution of an effective acoustic impedance values (Figs. 5 and 6) that characterize the section at a qualitative level (Vasil'ev and Urupov, 1978; Berzin et al., 2001). Estimations of effective acoustic impedance are interpolated on a cross-section, then smoothed out to a necessary degree vertically and horizontally and outputted in a colored form onto a section plane. In many cases, effective acoustic impedance sections allow not only to assess petrophysical relationships of contacting assemblages, but also present the structural information in a form that is more convenient for geological interpretation than the seismic reflection patterns, owing to the coherent continuous image of a geological medium. At the accepted dimension of depicted events as 400 m, the method made it possible to obtain detailed characteristics of the upper and middle portions of the Earth's crust down to 16–18 km depth.

Seismic data processing was undertaken, taking into account the seismic and geological features of a complex geological medium. Primarily, these features are as follows:

(1) a complex geometry of reflection boundaries;
(2) inhomogeneity of recorded seismograms as to frequency content and intensity related to changes in surface seismic and geological conditions; and
(3) high velocity values in the medium under study.

The CMP data processing flow incorporated the following procedures:

(1) installation of line geometry and inputting coordinates and elevations of profile points;
(2) common midpoint binning taking account of crooked line character;
(3) amplitude recovery and trace normalization;
(4) selection of gain control procedures to retain maximum record dynamics;
(5) noise rejecting;
(6) deconvolution of initial and stacked traces;
(7) determination of optimum stacking velocity;
(8) DMO-transform of CMP gathers;
(9) interactive automatic static correction for each stage of DMO correction;
(10) refining stacking velocity after DMO;
(11) band-pass filtering;
(12) post-stack migration; and
(13) time-to-depth conversion.

Particular attention was paid to the problem of static correction because static calculation accuracy fully defines the statistical effect of the CMP method. The 4B and 1-EU lines cross areas of different structures in the near-surface section. In the area under study, the near-surface section consists of Early Precambrian metamorphic and igneous rocks, which in some segments are heavily altered and overlain by glacial sediments.

In contrast to petroleum-bearing regions, where the static component is mainly contributed by the lowest velocity formation of the near-surface section, the weathering layer, the specific feature of the area under study is the inhomogeneity of the entire crustal section, for which the velocity and structural parameters essentially do not correlate with the parameters of the near-surface area. To compensate static distortions of seismic events, additional information about the structure of the near-surface section is necessary. Such information was obtained from special refraction sounding data. CMP gathers with first arrivals processed by special programs were also used, allowing velocity sections to be constructed to about 500 m depth.

To attenuate noise waves generated by the near-surface section and to increase the resolution of the reflection wavefield, one-dimensional and space-time filters were used. The parameters of these filters were calculated by taking into account limiting distortions to travel time and amplitude attributes of the desired signals.

Velocity selection to construct a CMP section and to conduct migration is an important issue. Continuous velocity analysis along a line incorporated obtaining vertical velocity spectra and velocity scan

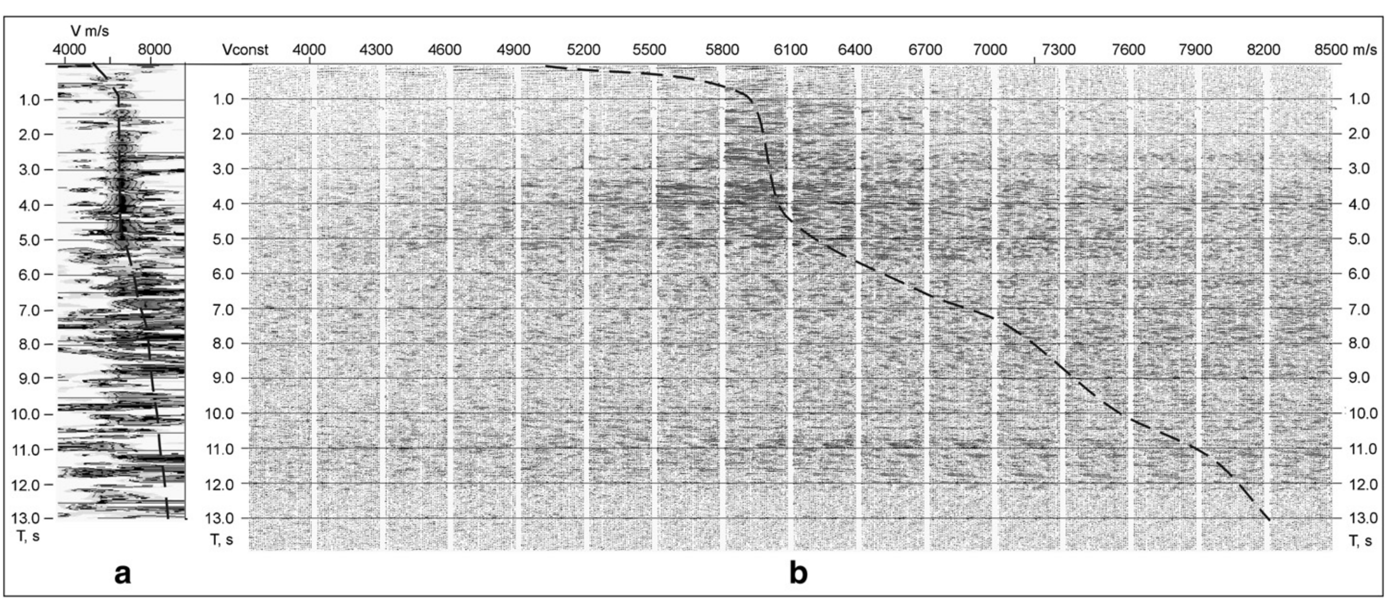

Fig. 4. Example of velocity analysis, line 4B, stake 68. a) Vertical velocity spectrum, b) constant velocity stack with 300 m/s interval.

with a 300 m/s step. The greatest velocity variations were obtained within the uppermost part of the section in the time interval up to 1.0 s where P-wave velocity ranges in value from 5.5 km/s to 6.1 km/s. For the time interval 1.0–5.0 s, a low gradient of increase in velocity with depth from 6.1 km/s to 6.4 km/s is usually typical. In the lower part of the section (>8 s), a change in the calculated velocity from 7.0 km/s to 8.5 km/s produces only a slight effect on the wavefield pattern. Vertical velocity spectra within the time interval 7.0–13.0 s have a blurred coherency peak (Fig. 4). There is no clear velocity contrast between crust and mantle over considerable distances.

Migration was carried out using the most typical model of velocity change with depth. This made it possible to obtain migrated CMP sections with dynamically expressed reflection boundaries within the entire time interval under study (Figs. 5 and 6).

4. Methods of geological interpretation of seismic images

Two rock types are predominant within the crust of the study region: (1) low-density and low-velocity gneisses and granitoids (2.58–2.8 g/cm^3 and 5.2–6.2 km/s correspondingly); and (2) high-density and high-velocity amphibolites (2.8–2.9 and up to 3.2 g/cm^3 and 6.0–7.2 km/s correspondingly) that rank much lower in abundance and make up thin (from a few centimeters to a few meters (Berzin et al., 2001)) lenticular bodies and layers that extend for tens and hundreds of meters (for a few kilometers in occasional cases). The amphibolites intercalating with amphibole and biotite–amphibole gneisses are often grouped into formations and members, up to a few kilometers in thickness. Metamorphic and migmatite banding on limbs of large folds reveals a roughly persistent trend, resembling the general stratification of the sequence as a whole that readily bends in compliance with the contours of large tectonic units.

The study of reflections in the crust consisting of metamorphic rocks indicates that the spectacular, surely identified packets of reflections may be in some cases reasoned by constructive interference of reflections from boundaries of relatively thin interlayers having a high acoustic impedance. The thickness of particular interlayers may be only a few decimeters, i.e., approximately 1/100–1/300 of wavelength (Ji et al., 1997). A representative section of such a geological medium was obtained from drilling the Kola Superdeep Well that penetrated a Neoarchaean gneiss–amphibolite–migmatite sequence from a depth of 6842 m down to 12,262 m at the borehole bottom. The migmatized gneisses and granites make up a matrix for nonuniformly embedded interlayers of dense, high-velocity amphibolite and meta-ultramafic interlayers varying in thickness from a few meters to 15–25 m and occupying approximately

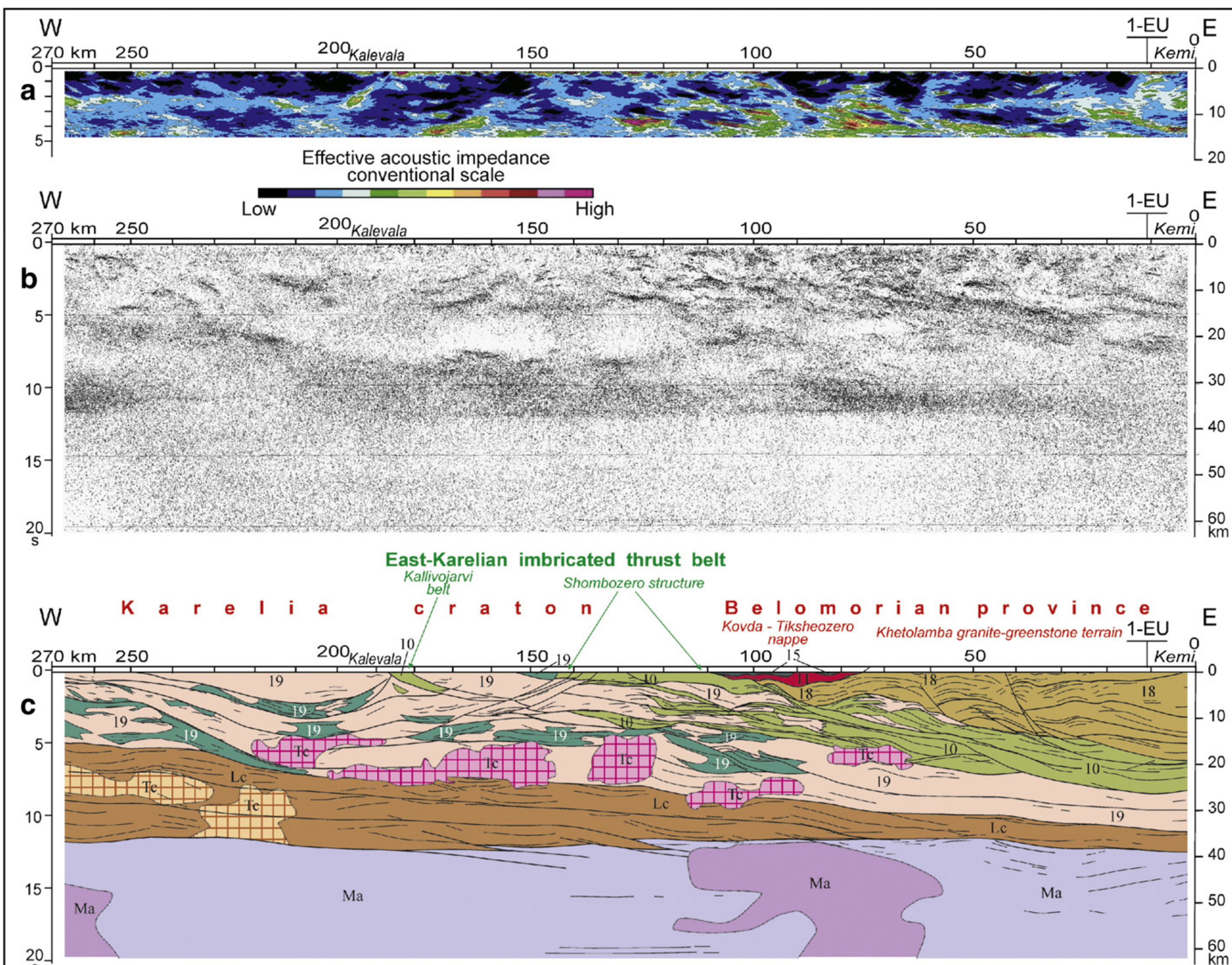

Fig. 5. The Earth's crust along cross-traverse 4B. a — Effective acoustic impedance section (a conventional scale is shown). b — Migrated CMP section. c — Geological model (see Fig. 1 for legend). The Archaean tectonic units are superscribed in red, the Palaeoproterozoic ones are in green; main units are superscribed in bold and local ones are in italic. (For interpretation of the references to color in this figure legend, the reader is referred to the web version of this article.)

20% of the section. The synthetic gathers (time sections), calculated along the Kola Superdeep axis (Mints and Stupak, 2001; Mints et al., 2004a) in order to estimate the role of thin amphibolite interlayers in creation of the seismic reflection pattern, have demonstrated the crucial contribution of interference from thin interlayers to the reflection pattern. It was found that degree of reflectivity within the section does not reveal a direct correlation with the number and dimension of geological bodies having petrophysical parameters that provide generation of effective reflections at their boundaries.

In geological interpretation of seismic data, we attached particular significance to the direct tracing of geological boundaries and fault zones recognized on the seismic reflection pattern and the section of effective acoustic impedance toward the day surface and to their correlation with mapped tectonic units. Comparison of the seismic image geometry with the geology of the southeastern Fennoscandian Shield at the present-day erosion level shows that the reflection pattern matches the general trends of compositional layering, gneissic banding, and schistosity. The roughly homogeneous structural domains of the crust correspond to relatively large tectonic sheets, 3–5 km thick. Their inner structure commonly is not discernible in reflection patterns. Regions with subtle reflections, and relatively low acoustic impedance were interpreted in agreement with day-surface geology as migmatised granite-gneiss complexes (e.g., assemblages within upper 2–3 km section around 200, 150, between 100 and 10-km stakes in 4B profile — see Fig. 5, also between 760 and 960-km stakes in 1-EU geotraverse — see Fig. 6). Large acoustically transparent domains are interpreted as granitoid or mafic plutons (see Figs. 5 and 6). The packets of extended reflections within bands having high acoustic impedance were interpreted as units of intercalating basic and acid volcanics and sedimentary rocks. Taking into account the packet morphology, they were referred to as (1) Palaeoproterozoic volcano-sedimentary sequences (extended bands that, reaching the surface, are directly tied up with Palaeoproterozoic belts and structures) and (2) Neoarchaean greenstone belts (mainly short and lenticular domains). It is evident that the correlation based on morphological features often remains tentative. Bodies with the highest acoustic impedance were regarded as being composed of mafic and ultramafic rocks (e.g., assemblages around 215 and between 150 and 110-km stakes in 4B profile — see Fig. 5, also at 890, 940 and 970-km stakes in 1-EU geotraverse — see Fig. 6).

5. Cross-section along the 4B profile

5.1. Seismic features

A detailed reflection pattern (Fig. 5-b) characterizes the crust and upper mantle from the present-day surface to a depth exceeding 60 km (more than 20 s). Reflection density varies over a wide range. No regular change in reflectivity rate is observed from upper to middle crust. The lower crust is characterized by strong near-parallel reflections of 3–5 km extent, dipping slightly eastwards. The upper boundary of the region of low-crustal reflections at the western end of the profile is at a depth of some 15 km and dips eastwards. From DSS data, velocities (V_p) in the lower crust increase from about 6.8 km/s in its upper part to 7.0 km/s near the Moho discontinuity (Berzin and Pavlenkova, 2001). However, the DSS boundaries coincide with upper and lower boundaries of the reflectivity zone very roughly and these figures make very approximate estimates only.

The subhorizontal crust–mantle boundary at 39 km depth is indicated by a sharp reduction in the number and extent of reflections. Towards the eastern end of the profile it dips very gently, reaching a depth of 40 km. On segments where the lower crust is characterized

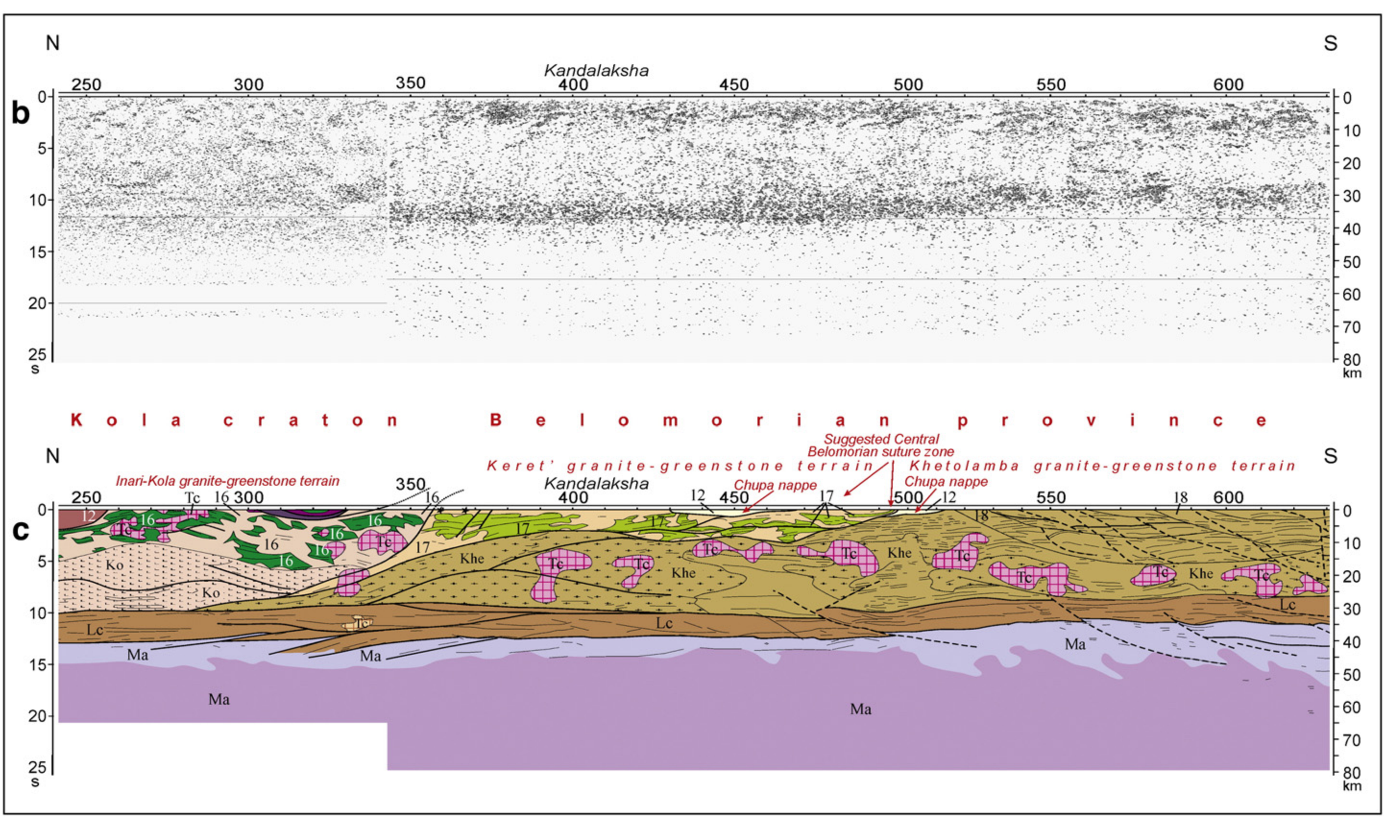

Fig. 6. The Earth's crust along geotraverse 1-EU. a — Effective acoustic impedance section (a conventional scale is shown). b — Migrated CMP section. c — Geological model (see Fig. 1 for legend). The Archaean tectonic units are superscribed in red, the Palaeoproterozoic ones are in green; main units are superscribed in bold and local ones are in italic. (For interpretation of the references to color in this figure legend, the reader is referred to the web version of this article.)

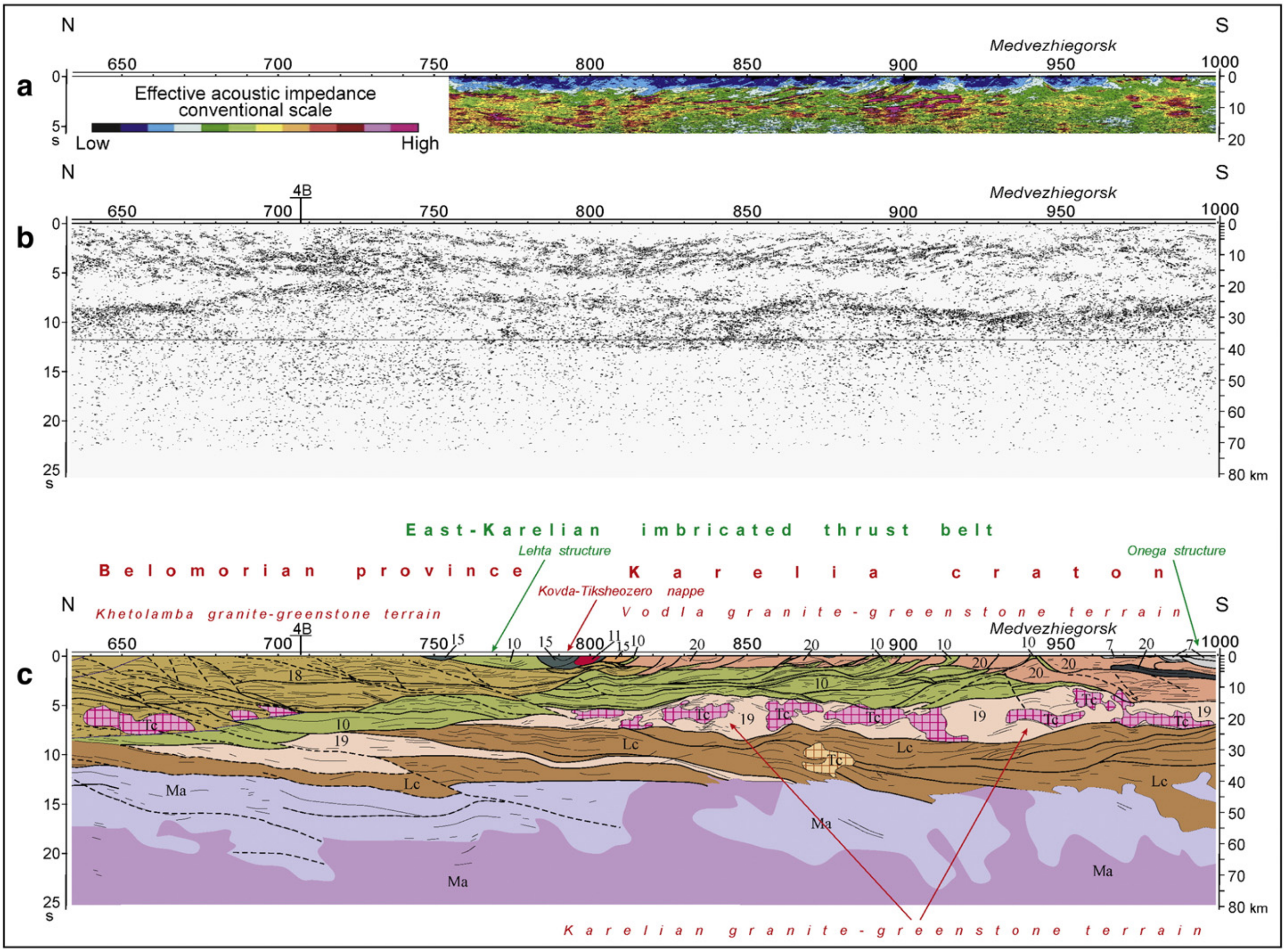

Fig. 6 (*continued*).

by reducing reflection bin density, the crust–mantle boundary is almost indiscernible. For the mantle, relatively sparse reflections of small extent are typical, forming a group within the limits of the near-horizontal zone at a time of 20–22 s (Mints et al., 2004a; Sharov, 2004). An increase in the number and extent of reflections in the adjacent part of the mantle is related to crustal thinning. A weakly expressed reflection pattern makes it possible to trace crustal structures into the mantle (Fig. 5-b).

Reflections in the middle and upper crust form distinct groups indicating, with some interruption, structural domains of 10–100 km extent and thickness from 1 km to about 4 km (Fig. 5-b). In the middle part of the profile, in the interval 150–85 km, transparent or semi-transparent, oval- and lens-shaped regions of 10–30 km extent and 1.5–3.0 km thick are contained within intervals between smoothly curved linear domains. These regions are filled by chaotically oriented or partly ordered short reflections. Crustal areas in the eastern and western parts of the profile are separated by a zone of extended strong reflections that can be traced, with a small break, from the surface (120–110 km interval) down to a depth of 20–23 km. Its eastern continuation is outside the profile. The seismic image of the crust over this zone (interval 110–0 km) is formed by smoothly curved reflection groups with an insignificant number of semi-transparent regions between them (Fig. 5-b).

The effective acoustic impedance section from the day-surface to a depth of 15 km (Fig. 5-a) shows a combination of oval or lenticular regions characterized by low values of acoustic impedance and relatively thin zones with increased and high values of acoustic impedance. As a rule, zones of increased acoustic impedance conform to clearly expressed wavetrains. On the contrary, regions of low acoustic impedance are usually associated with areas of increased transparency, although separate well-expressed wavetrains are also contained within such regions. The zone of high acoustic impedance referred to above conforms to a zone of extended strong reflections. Near-surface features characterized by increased acoustic impedance are compared with mapped amphibolite and basalt bodies as well as with local positive anomalies of gravity and magnetic fields. Regions of decreased acoustic impedance in turn are correlated with granite, granite-gneiss and migmatite.

5.2. Structural–geological interpretation

A model of deep crustal structure (Fig. 5-c) is based on correlation between the seismic reflection pattern, acoustic impedance distribution, and rock assemblages shown on the regional geological map (Fig. 1). This approach allowed tracing the geological boundaries mapped at the surface to considerable depths, in some cases to the crust–mantle boundary. The basic feature of the crustal section studied consists in a distinct layering on both the level of "transparency-reflectivity" and the nature of the structural pattern. Most of the layers, varying somewhat in thickness, gradually dip down towards the eastern end of the profile.

Strongly reflecting lower crust becomes significantly thinner eastwards, approximately from 20 km to 5 km. A tectonic sheet about 16 km thick at the western end of the profile covers the lower

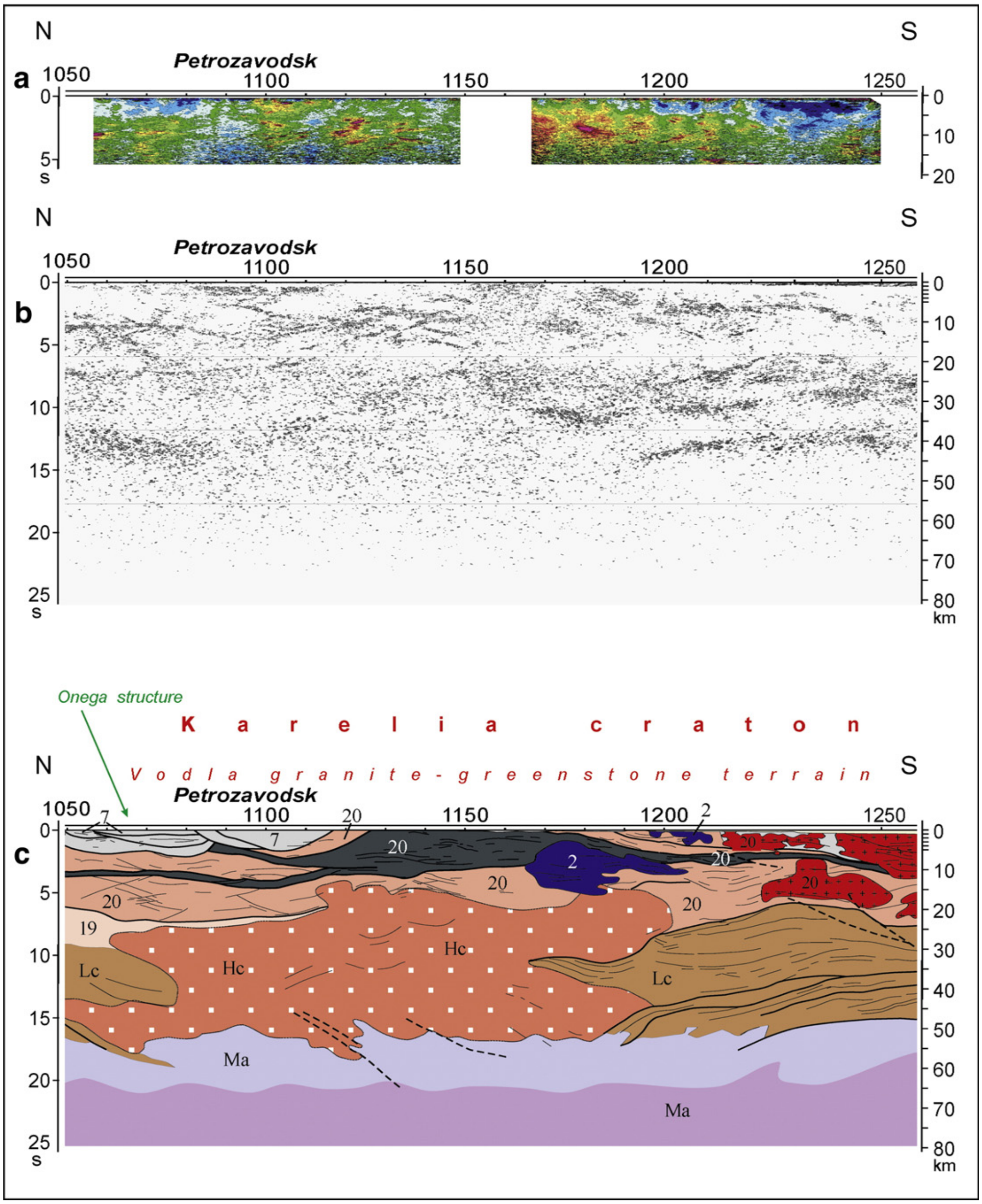

Fig. 6 (*continued*).

crust. It is approximately 30–35 km thick in the central part of the profile and then becomes 10–12 km thick to its eastern end. Acoustically transparent oval-shaped regions within this sheet associated with interval between stakes 175 km and 115 km probably mark the location of large intrusive bodies.

The base of the sheet-like crustal region lying higher in the section reaches the present-day surface between the 190 km stake and the western end of the profile. The sheet dips towards the eastern end of the profile, slightly decreasing in thickness, where it occurs at a depth of 26–37 km. On the surface, this sheet is represented by uniform leucocratic medium- and coarse-grained plagioclase gneisses (high-alumina trondhjemite gneisses). Gneissosity and banding of migmatites dip steeply southwestwards in conformity with the orientation of the reflection events. Coarse- and medium-grained biotite and amphibole-biotite gneisses with lenses of fine-grained biotite gneisses and amphibolites crop out on the profile segment 225–205 km.

Thus, the crust within this part of the section is formed by a combination of tectonic sheets, which dip eastwards gradually flattening out. Neoarchaean rocks of the Karelian granite-greenstone terrain form the upper sheet. Apparently, the sheet occurring below is also formed by rocks of the same type. It reaches the surface in Finland in the vicinity of the Kuhmo–Suomussalmi greenstone belt.

A clearly detected inclined sheet, marked by the zone of strong reflections noted above, is formed by rocks of increased and high acoustic impedance (Fig. 5-a). In the 4B section it separates the Belomorian province from the Karelia craton and consists of a series of structurally uniform domains of 5–6 km total thickness. In the upper crust, starting at 15 km depth, the structural domains split, forming a fan consisting of 3–4 individual sheets diverging westwards (Fig. 5). The upper sheet 2 km thick is folded into a gentle antiform and is cut by the present-day surface. Its boundaries coincide with those of the Palaeoproterozoic Shombozero structure. This sheet comprises Palaeoproterozoic sedimentary-volcanic rocks. It can be assumed that rocks of the same type, which have a similar seismic pattern and petrophysical parameters, form the underlying tectonic sheets in this fan. Field observations indicate that the central part of the Shombozero structure consists predominantly of shales and metabasalts dipping northeastwards at gentle and moderate angles on the eastern limb. Further to the west, the Kallivojärvi structure forms one of the tectonic sheets in the above-mentioned fan. Within it, shales, quartzitic sandstones and basalts dip vertically or steeply westwards.

We have called the tectonic ensemble formed by alternating tectonic sheets of Neoarchaean granite-gneisses and Palaeoproterozoic rocks the East-Karelian imbricate thrust belt. Oval and lenticular shapes of the granite-gneiss segments, as well as their "intrusions" into the linear Palaeoproterozoic structures, indicate probable partial melting and movement of rocks of granitic composition, accompanied by deformation of Palaeoproterozoic assemblages.

On the profile segment of 80–60 km, an asymmetric antiformal fold is clearly observed in the upper part of the crustal section, immediately adjacent to the upper boundary of the tectonic assemblage of the East Karelian imbricate thrust belt (Fig. 5). The fold consists of rocks with increased acoustic impedance, similar to rocks of the Palaeoproterozoic sedimentary-volcanic complex. Alternatively, it may belong to Belomorian province. The morphology of the folded sheet structure indicates on the whole that it formed during thrusting, accompanied by the formation of structural duplexes riding "piggy back" in sequence, and piling up of displaced tectonic sheets that were deformed into antiformal folds.

The upper part of the crust in the eastern section of the profile (110–0 km) belongs to the Belomorian province. Its constituent geological associations are thrust over the East-Karelian imbricate thrust belt. At the same time, the morphology of the folded structures indicates subsequent subsidence of the crust of the Belomorian province, accompanied by the transformation of thrusts into normal faults. An analysis of the reflection pattern and the section of effective acoustic impedance makes it possible to detect several tectonic sheets in the section of the Belomorian province. The uppermost Kovda–Tiksheozero sheet (Kovdozero tectonic nappe of Miller, 2002), is formed by the granite-greenstone association including the Tikshozero, Keretozero and Hizovaara greenstone belts and enderbites, charnockites, migmatites and granite-gneisses. The Kovda–Tiksheozero sheet is underlain by the Khetolamba terrain, formed of rocks with decreased acoustic impedance, probably gneisses or granitic rocks, and increased acoustic impedance, probably amphibolites. Strong reflections more characteristic of rocks with increased acoustic impedance have an affinity with the lower crustal association (Fig. 5).

6. Cross-section along the 1-EU geotraverse, 250–1250 km

6.1. Seismic features

The base of the crust, the crust–mantle discontinuity, is clearly detected at depths of 37–40 km in the northern segment, 40 km in the central part, and 42–45 km in the southern segment of the profile (Fig. 6). A smoothly curving top of the lower reflectivity zone can be traced within the 20–30 km depth interval except in the central part (650–750 km) where it is around 35 km. In contrast to the 4B profile, the crust–mantle discontinuity is characterized by very significant variations in both depth and structure. In the northern segment, 250–830 km, it is represented by a clearly traceable, almost horizontal surface at 40 km depth. This agrees with the 4B profile, which intersects the geotraverse 1-EU near the 700–708 km interval (10–15 km on line 4B respectively). Starting from 850 km, the crust–mantle has serrated outlines distinct in some places and ill-defined in others. Similar features of the crust–mantle boundary are characteristic for the short interval between 300 and 350 km. The structural shape of the reflection pattern in the lower crust conforming to the "serrated" form of the crust–mantle boundary indicates subsidence of lower-crustal fragments into the mantle (Fig. 6).

A strongly reflecting lower crust can be traced along the greater part of the profile excluding the 650–750 km segment. As in line 4B, the crust–mantle boundary is discontinuous or poorly discernible where the lower crust is characterized by increased transparency. The thickness of the low-crustal reflectivity zone is around 8–10 km between 250 and 650 km, significantly thinner at 650–740 km and then becomes 20 km thick and more at the southern end of the profile. The parts of the mantle directly underlying the «serrated» crust–mantle boundary are distinguished by the presence of irregularly distributed, in part rather strong reflections. In a sense this zone may be interpreted as a "crust–mantle mixture". Alternatively, this zone may consist of mafic eclogite-facies rocks of crustal affinity.

The major break in the crust–mantle boundary in the 650–750 km geotraverse interval is related to subsidence of the crust into the mantle (Fig. 6). Some indications of such a break can be observed at the eastern end of the 4B profile near its intersection with the 1-EU geotraverse. The nature of the crustal "layers" near the crust–mantle boundary – a sharp thinning of the lower crustal "layer" and the appearance of reflections in the adjacent mantle – have already been referred to. It should be noted that breaks in the crust–mantle boundary are almost everywhere accompanied to some extent by an increase in the number of reflections in the adjacent part of the mantle. As in line 4B, the reflection pattern makes it possible to trace portions of the crust into the mantle, as well as to correlate structural features of seismic images of the lower crust with adjacent mantle. Matching of seismic images noted by observations on independent shot profiles is important evidence that we are dealing with a real, natural phenomenon, rather than artifacts arising from instrumental factors in the seismic methodology.

The distribution of reflectors in the middle and upper crust is broadly similar to that observed along profile 4B. Boundaries of similar domains are smoothly curved lines, defining complex features of crustal structure. An important feature is the presence of extensive (a few hundred kilometers long) structural domains 1–2 to 5–6 km thick, formed by zones of strong parallel reflections, which in places are clustered to form wavetrains of more significant thickness (Fig. 6).

6.2. Structural and geological interpretation

The lower crustal "layer", where it is defined, dips southwards. It is characterized by the thickness varying from 8–10 km to 30 km. Within the intervals 300–350 km and 850–1000 km, the structural pattern indicates bending and dipping of separate, finely laminated crustal slabs into the mantle, where they reach a depth of 52–55 km. In isolated cases, we succeeded in tracing reflections marking this dip of lower crustal slabs into the mantle and their disintegration and "dissolution" within the mantle down to about 70 km depth (Fig. 6-c). Features of the lower crustal boundary indicate considerable lateral displacements along this discontinuity, accompanied by deformation of lower crustal and mantle rocks and subsidence (subduction) of a delaminated crustal slab. On the 1-EU geotraverse segment 750–850 km, the lower crustal slab contains a "transparent" sheet-like body 3–4 km thick. Comparison with the section along the 4B profile makes it possible to assume that it must be one of the tectonic sheets formed by the granite-greenstone complex of the Karelia craton (Figs. 5 and 6). As mentioned above, the major break in the crust–mantle boundary in the 650–750 km 1-EU geotraverse is related to subsidence of the crust into the mantle also (Fig. 6). This phenomenon may be related to collisional crustal thickening.

Along 300–650 and 750–1000 km intervals the lower crust is overlain by a significantly transparent crustal sheet clearly bounded top and bottom in the north and central parts of the geotraverse portion under consideration. The seismic image of this sheet within the 800–1000 km interval and its location within the crustal section

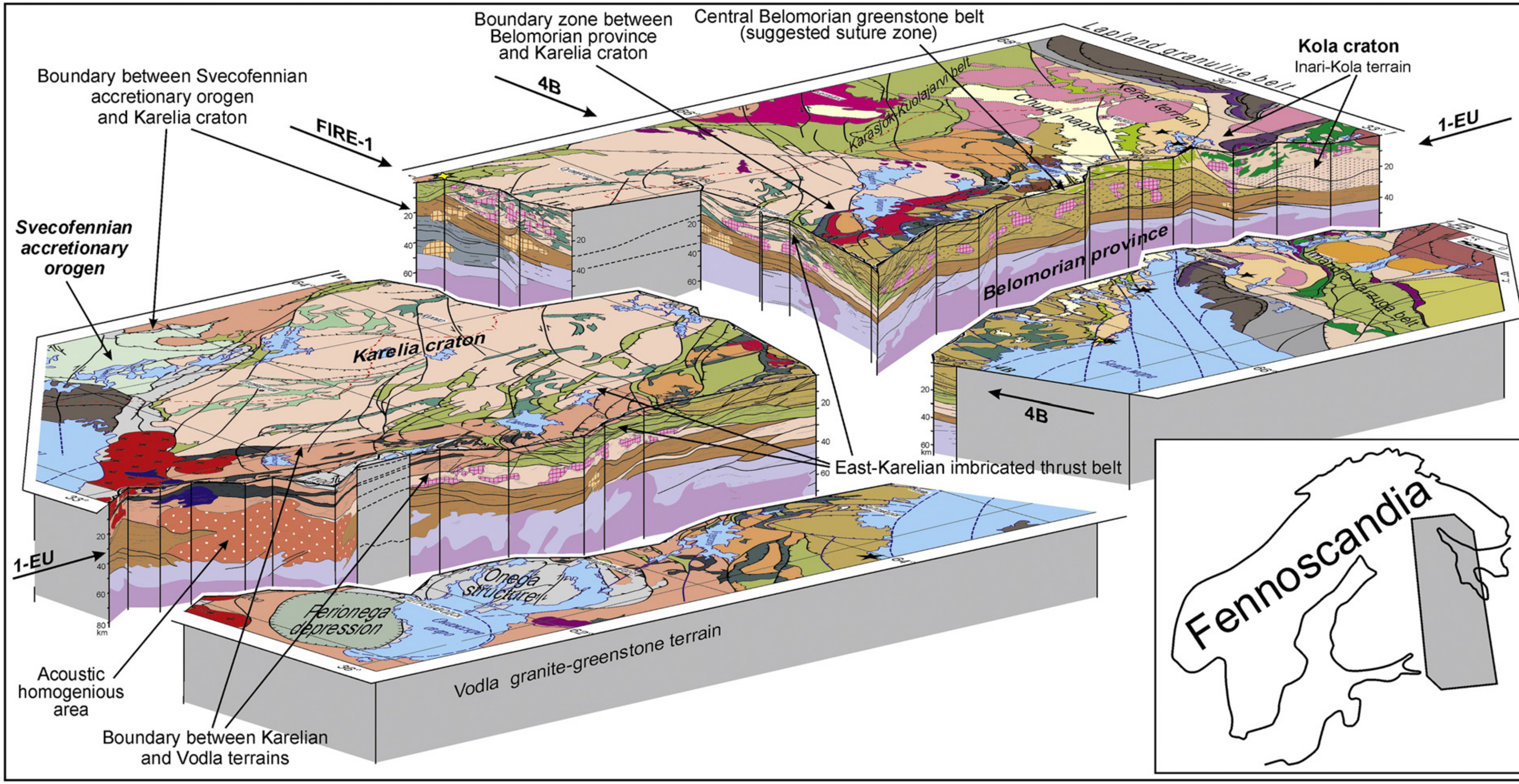

Fig. 7. Three-dimensional image of the Earth's crust under the southeastern Fennoscandian Shield showing the geological interpretation of the seismic reflection images superimposed on the geological map. See Fig. 1 for legend.

make it possible to compare it reliably with the crustal sheet formed by rocks of the Karelian granite-greenstone complex and detected on the section along the 4B profile. Its structure is characterized by an alternation of segments with consistent thickness of the order of 7–8 km, and swells reaching a thickness of 10–12 km. The lower boundary of the sheet intersects at a low angle elements of the lower crustal lamination, indicating the tectonic nature of this boundary.

Within 350–650 km and further to 810 km stake the geotraverse crosses the Belomorian province (Figs. 1 and 6). The variably reflecting crust above the lower reflectivity zone belongs to the Khetolamba granite-greenstone terrain. In contrast to the Karelian terrain in the 4B section, there are much more reflective domains, but their boundaries are more diffuse. It seems conceivable that alternating greenstones, gneisses and granite bands and lens-shaped bodies form the Khetolamba crust. Within the interval 470–500 km, the 1-EU profile crosses the Central-Belomorian greenstone belt (see Figs. 6 and 7 for location). The reflection image in agreement with the geological mapping data evidences a subsidence of tectonic sheet northwestward, first rather gently, then more steeply farther north. The TTG-gneisses hosting the greenstone assemblages include the above-mentioned eclogite bodies. After significant thinning this complex granite-greenstone eclogite-bearing sheet plunges beneath the crust of the Kola craton. The Chupa tectonic nappe formed of kyanite gneisses has a restricted thickness, less than 4 km, in the 1-EU section.

From the 930 km stake southwards, within the upper part of the crustal section, another sheet about 5 km thick is detected. This sheet is comparable with the Vodlozero granite-greenstone complex formed by the oldest granite-gneiss and sedimentary-volcanic assemblages of the Fennoscandian Shield (Fig. 6).

The upper crustal structure, part of the East-Karelian imbricated thrust belt, is of special interest in the 1-EU geotraverse interval of 800–940 km (Fig. 6). The pattern of seismic reflections and the effective acoustic impedance section allow the identification of discrete thin sheets formed by rocks of the Palaeoproterozoic volcano-sedimentary and Neoarchaean granite-gneiss complexes. Interleaving of separate sheets and packages formed by rocks of both complexes indicates their transport southward (in modern coordinates) during tectonic displacement. The upper crustal structure in the southern part of the geotraverse portion under consideration is a thrust–nappe structure of opposing vergence (Mints et al., 2004b). Coincidence of both directions of tectonic transport occurs near the profile interval 940–945 km where the profile crosses two zones formed by basaltic lavas that have been brought together (Fig. 6). Between these zones, granitoids and migmatites of Neoarchaean age are exposed.

It is noteworthy that an increase in the thickness of the upper crust connected with sheet clusters intimately coincides spatially with the region of increased thickness of the lower crust and sinking of segments of it into the mantle (Fig. 6). It is important to note that both packages, the first formed by upper crustal Palaeoproterozoic volcano-sedimentary assemblages, the second by low-crustal sheets, verge in opposite directions.

7. Discussion: 3D model of the crust and upper mantle structure

Careful coordination of mapped surface geological structures and geological interpretation of the seismic images along both seismic cross-sections enabled a detailed interpretation of the 3D model (stereometric section representation) of the Earth's crust and upper part of the lithospheric mantle in the studied region. Additional information was provided by the recently published seismic data along the FIRE-1 profile in Finland (Korja et al., 2006; Kontinen and Paavola, 2006). These data were partially reinterpreted by us and used in the western part of the 3D model (Fig. 7).

In Figs. 5–7, thrust zones and imbrication of the sheets and slices formed by the Neoarchaean and Palaeoproterozoic rocks are clearly identifiable. It is easy to see that gently dipping tectonic sheets up to several hundred kilometers long, formed of both Archaean and Palaeoproterozoic assemblages, can be traced below the present-day surface, in some cases as far as the crust–mantle boundary, where irregularly distributed reflection events continue the main trends of the crustal structure down to the mantle. The Neoarchaean terrain that has for long been considered as a system of "blocks" of crustal dimensions, characterized by individual subhorizontal layering (e.g., Sharov, 1997; Korsman et al., 1999), appears as an assemblage formed by inclined crustal sheets and slices. The tectonic slices within the Belomorian Province in contradistinction to above mentioned model of Bibikova, Slabunov and co-workers (Bibikova et al., 1999; Slabunov, 2005; Slabunov et al., 2006) plunge northeastward beneath the Kola craton.

7.1. The lower crust, mantle, and crust–mantle discontinuity

The regular change of thickness is the principal feature of the mainly high-reflective but locally semi-transparent lower crust. The maximum thickness of the stakeed lower-crustal slices, up to 25–30 km (FIRE-1 and 1-EU profiles), is characteristic for the marginal areas of the Karelia craton at its boundary with the Palaeoproterozoic Svecofennian accretionary orogen. The lower-crustal slice thins with distance from this boundary. Beneath the Belomorian province and Inari–Kola terrain its thickness is around 8–10 km. It is seen clearly from the 4B and FIRE-1 sections that the overlying slice formed by granite-greenstone assemblages was displaced and inclined after an origin of granitoid plutons (the acoustically transparent areas) related to Neoarchaean collision. These specifics lead to the conclusion that the present-day lower crust was generally formed as a result of the accretion of mafic oceanic crust during the Palaeoproterozoic. Alternatively, it could have been created in the Archaean, but deformed and stakeed during the Palaeoproterozoic. The best case for an Svecofennian provenance of the stakeed lower-crustal slices can be made for the 275–175 km interval of the FIRE-1 profile (only the eastern flank of this profile is shown in Fig. 7). According to our analysis of the seismic images (see App. 2 and 3 in Kukkonen and Lahtinen, 2006), the Svecofennian mid- and lower-crustal slices of island-arc and/or oceanic affinity can be directly traced from the present-day surface at Kiuruvesi (275th km) to Kuhmo (50th km) area where they "dissolve" in the mantle. The total thickness of the stakeed mid-lower crust in this section reaches 30–35 km.

The composition of the lower crust and the nature of the crust–mantle boundary (approximately the Moho) beneath Precambrian shields so far remain a matter of debate. Geophysical data and deep xenoliths indicate that the lower crust consists largely of basic rocks metamorphosed in granulite to eclogite facies (Rudnick and Fountain, 1995). The lower crust of the Belomorian province is characterized by entrained xenoliths in Devonian lamprophyre and kimberlite dykes and pipes on the White Sea coast and offshore islands. The xenoliths are composed of Neoarchaean and Palaeoproterozoic gabbroic rocks and gabbro-anorthosite transformed during the Palaeoproterozoic into garnet granulite and high-T eclogite (or high-P granulite) (Kempton et al., 2001). The density of xenoliths varies from 3.0 to 3.6 g/cm^3, and V_p value is within the range 6.8–7.9 km/s (Markwick and Downes, 2000). The mantle-derived xenoliths consist of spinel peridotite that crystallized at the same depth as lower crustal rocks (Vetrin, 2006; Mints et al., 2007). The measured density of granulites from the lower crust beneath the Belomorian province is comparable with the world average density of lower crustal garnet granulites, garnet-bearing anorthosites, and upper mantle eclogites (3.00–3.28, 2.79–3.06, and 3.24–3.59 g/cm^3, respectively). The respective V_p values are 7.03–7.50, 7.26–7.55, and 7.71–8.58 km/s (Rudnick and Fountain, 1995).

The velocity and density of crustal and mantle rocks beneath the Karelian Craton along the GGT-SVEKA Geotransect in Finland were estimated as 6.88–7.09 km/s in the lower crust, 8.20 km/s in the upper mantle immediately under the Moho discontinuity, and up to 8.42 km/s at a depth of about 60 km; the upper mantle densities are 3.10 and 3.48 g/cm^3, respectively (Korsman et al., 1999). Similar estimates were obtained along the Kem'-Ukhta profile: 6.8–7.0 in the lower crust and 8.0 km/s in the upper mantle adjacent to Moho (Berzin and Pavlenkova, 2001). Taking into account the trends of regional geological structures (Fig. 1), we suggest that the Devonian dykes and pipes located close to the 400 km stake of the 1-EU geotraverse brought up xenoliths from just this depth level. Summarizing the available information, one can state that the lower crust and upper mantle (at least, above the reflection boundary traced to a depth of ~60 km between 150 and 110 km of the 4B section) consist of high-grade mafic rocks associated with spinel peridotite that appears below a certain depth. The ultramafic rocks proper (without a substantial amount of basic rock) are thought to occur beneath the aforementioned reflection boundary. The lower crustal sequence characterized by compositional layering and a wide variation of acoustic impedance may be correlated with the Bergen Arc gabbro-anorthosite–granulite–eclogite sequence in Norway displaying effective reflectors at granulite–eclogite contacts. The Bergen Arc sequence is considered to be a typical example of layered lower crust (Fountain et al., 1994). The upper part of the mantle ("crust–mantle mixture") intersected by the 1-EU and 4B profiles consists possibly of relatively uniform eclogite or an association of eclogite and spinel peridotite devoid of strong reflections at the boundaries between both types of rocks. The geological data together with petrological estimates of the depth of metamorphism of the xenoliths, leads to the conclusion that lower crustal rocks occur beneath the present-day Belomorian province at a depth of at least 50 km (Mints et al., 2007). At the same time, as follows from the DSS results, the depth to the Moho (upper boundary of high-dense eclogite) does not exceed ~40 km (Sharov, 1997).

The age of the earliest granulite-facies metamorphism of the lower-crustal xenoliths is poorly constrained. Plagioclase — whole rock Pb–Pb data suggest two main metamorphic events during the Palaeoproterozoic at ~2.4 Ga and ~1.8 Ga (Neymark et al., 1993). Also, a Pb–Pb isochron age of 2.6 Ga has been obtained for the earliest garnet crystallization in the granulite xenoliths; a concordant U–Pb age of garnet in one of the analyzed samples is 2.59 Ga (Kempton et al., 2001). Some zircon grains yield ages at 2.84 Ga (Downes et al., 2002) and 2.71 Ga (Arzamastsev et al., 2000). Thus, at least part of the lower crust beneath the Belomorian province had been created by the end of the Archaean (Vetrin, 2006 and references therein).

The structure of the lower crust and the crust–mantle discontinuity indicates that this fundamental boundary bears not only a compositional but also a tectonic character. In particular, the wedging-out of the lower crust along with the eastward plunge of the assembled tectonic sheets indicates a large-scale displacement and deformation of the lower crustal layer accompanied by slip along the crust–mantle discontinuity. Thus, the detailed pattern of seismic reflections and their structural interpretation provide evidence of the tectonic origin of the crust–mantle boundary, which is apparently a thick zone of tectonic flow and displacement of large crustal sheets, accompanied by the sinking of individual lower crustal segments into the mantle. The crust–mantle discontinuity was subsequently intruded by the mantle-derived magmas.

7.2. Crustal structure

The Karelian granite-greenstone terrain appears as a wedge-shaped crustal slice with a maximum thickness of approximately 30 km that thins eastward beneath the Khetolamba terrain. The latter is the main constituent of the Belomorian crust, which is thrust westward over the Karelian terrain. The southeastern margin of the Karelian terrain is overthrust by the ancient Vodla terrain. The Khetolamba terrain in turn plunges beneath the Inari–Kola granite-greenstone terrain. Eclogite-hosting TTG-gneisses of the Keret' terrain sandwiched between both above mentioned units were traditionally understood as one of the main constituents of the Archaean Belomorian province (e.g., Slabunov et al., 2006). However, not prominent in the seismic image, this boundary may be regarded as the main Neoarchaean collision zone. Its importance derives from the numerous eclogite inclusions that evidence the long-lived subduction of oceanic lithosphere (at least from 2.86 and possibly up to 2.70 Ga). Deep crustal structure of the area formed by succession of tectonic plates and slices made (upwards from below) of Khetolamba terrain — Central Belomorian greenstone belt — Keret' eclogite-hosting TTG-gneisses — Inari–Kola terrain can be considered as a remnant of the great orogenic belt resulted from collision between Karelia and Kola cratons. In such a scenario Central Belomorian greenstone belt plays a role of suture and Keret' terrain must be understood as an active margin of the Kola craton. Exhumation of the eclogite-bearing lower crustal section could be the result of the collision at approximately 2.7 Ga. However, data on eclogite facies metamorphism of the Palaeoproterozoic dykes that cut the Keret' tectonic nappe (Volodichev et al., 2004; Dokukina et al., 2006) strengthens the assignment of a Palaeoproterozoic age to the exhumation of the Keret' granite-gneiss assemblage as well as to the Archaean and Palaeoproterozoic eclogites that were originally emplaced at the same lower-crustal level.

The Palaeoproterozoic East Karelian imbricated thrust belt is separated from the underlying sheet by a major detachment. This surface is located at a depth of 10–15 km, dipping to 27 km at the intersection of geotraverse 1-EU and cross-traverse 4B. The morphology of the deformed tectonic sheets in the crust of the eastern Karelian terrain is the result of the imbrication and thrusting of these sheets in western and southwestern directions. Repeated reverse and thrust faulting and the formation of structural duplexes accompanied tectonic transport. The origin and evolution of the Svecofennian accretionary orogen along the southwestern margin of the Karelia craton, which occurred in the late Palaeoproterozoic, resulted in creation of complex collision type structures. Northeastward subduction and underthrusting of the thick crustal slices formed by the oceanic, island-arc and back-arc assemblages was accompanied by overthrusting of the upper-crustal tectonic sheets of the same vergence (see sections along FIRE-1 and 4B sections in Fig. 7). The resulting crustal structure has features typical of convergent collision orogens with characteristic tectonic wedge development (Moore and Wiltschko, 2004). This understanding coincides in main lines with geological sections across the Svecofennian lithosphere suggested earlier from the BABEL profiles (e.g., BABEL Working Group, 1990, 1993; Öhlander et al., 1993; Abramovitz et al., 1997).

The crustal structure inferred for the southeastern Fennoscandian Shield is clearly comparable with other segments of Early Precambrian crust studied in detail by the CDP method, such as the Canadian Shield (Baird et al., 1996; Cook et al., 1998; Eaton and Hynes, 2000; Eaton et al., 2000; Ludden and Hynes, 2000; Jackson, 2002; Cook et al., 2004) and Kaapvaal Craton (De Wit and Tinker, 2004).

8. Conclusion

The model of the crustal structure of the southeastern Fennoscandian Shield developed here offers a number of improvements to existing concepts. However, further refinement of the model requires additional discussion of a wide range of geological, geochemical, geochronological and petrological data beyond the bounds of the present paper.

In summary:

(1) Geological interpretations of seismic data obtained from investigations along the northern part of 1-EU seismic geotraverse and cross-line 4B across the Karelian granite-greenstone terrain, the southern part of the Belomorian belt and a

number of Palaeoproterozoic sedimentary-volcanic belts, together with results of geological mapping, provide evidence that the Early Precambrian crust is characterized by north-eastward inclined structural layering.

(2) The crustal architecture is a combination of thrust–nappe and thrust–underthrust structural assemblages formed by both Neoarchaean and Palaeoproterozoic rocks that were additionally deformed during uplift and emplacement (bulging) of granite gneiss domes.

(3) Formation of the inclined structural assemblages resulted from the Neoarchaean subduction and collision processes (~2.9–2.5 Ga) and Palaeoproterozoic collision events (2.5–1.6 Ga).

(4) The new model of the structure of the Early Precambrian crust substantially modifies previous concepts of the crust of the eastern part of the Fennoscandian Shield as being composed of blocks with subvertical boundaries and individual internal layering. It is apparent that the traces of gently dipping boundaries on the surface are a function of the level of erosion and, as a consequence, such boundaries cannot be considered as defining blocks in the traditional sense.

(5) The detailed pattern of seismic reflections and their structural interpretation in the lower crust provide evidence of the tectonic origin of the crust–mantle boundary, which is apparently a thick zone of tectonic flow and displacement of large crustal sheets, accompanied by the sinking of individual lower crustal segments into the mantle.

Acknowledgments

Seismic study along the 1-EU and the 4b profiles was accomplished under the Program of Deep Crustal Studies of the Russian Ministry of Natural Resources. This paper was delivered at the SEISMIX 2006 Conference in Hayama, Japan and forms a contribution to the IGCP-474 project. Authors thank the RFFI (project No. 05-05-65012) for financial support of the research and IGCP-474 Project for funding that permit authors to take part in the conference. Special thanks to Randell Stephenson for helpful comments and Thomas Frisch for improving the English text.

References

Abramovitz, T., Thybo, H., Berthelsen, A., 1997. Proterozoic sutures and terranes in the southeastern Baltic Shield interpreted from BABEL deep seismic data. Tectonophysics 270, 259–277.

Arzamastsev, A.A., Belyatsky, B.V., Arzamastseva, L.V., 2000. Agpaitic magmatism in the northeastern Baltic Shield; a study of the Niva intrusion, Kola peninsula, Russia. Lithos 51, 27–46.

BABEL working group, 1990. Evidence for early Proterozoic plate tectonics from seismic reflection profiles in the Baltic Shield. Nature 348 (6296), 34–38.

BABEL working group, 1993. Integrated seismic studies of the Baltic Shield using data in the Gulf of Bothnia Region. Geophys. J. Int. 112, 305–324.

Baird, D.J., Nelson, K.D., Knapp, J.H., Walters, J.J., Brown, L.D., 1996. Crustal structure and evolution of the Trans-Hudson orogen: results from seismic reflection profiling //. Tectonics 15 (2), 416–426.

Balashov, Yu.A., 1996. The Palaeoproterozoic geochronology of the Pechenga–Varzuga structure. Petrology 4 (1), 1–22 (in Russian).

Bayanova, T.B., 2004. An Age of the Datum Mark Geological Complexes of the Kola Region and Duration of the Magmatic Processes. Nauka, S.-Petersburg. 174 p.

Berzin, R.G., Pavlenkova, N.I., 2001. A comparison of reflection and refraction data on the Kem'-Ukhta profile. In: Sharov, N.V. (Ed.), Deep Structure and Evolution of the Earth's Crust in the Eastern Fennoscandian Shield: Kem-Kalevala Profile. Karelian Sci. Center, Russian Academy of Sciences, Petrozavodsk, vol. 64–77 (in Russian).

Berzin, R.G., Suleimanov, A.K., Zamozhnyaya, N.G., Andryushchenko, Yu.N., Stupak, V.M., 2001. Geophysical investigations on regional profile 4B. In: Sharov, N.V. (Ed.), Deep Structure and Evolution of the Earth's Crust in the Eastern Fennoscandian Shield: Kem-Kalevala Profile. Karelian Sci. Center, Russian Academy of Sciences, Petrozavodsk, vol. 39–63 (in Russian).

Bibikova, A.I., Slabunov, A.I., Bogdanova, A.I., Sciold, T., Stepanov, V.S., Borisova, E.Yu., Kevlich, V.I., 1999. Early magmatism of the Belomorian Mobile Belt, Baltic Shield: lateral zoning and isotopic age. Petrology 7 (2), 123–146.

Bibikova, E.V., Bogdanova, S.V., Glebovitsky, V.A., Claesson, S., Skiold, T., 2004. Evolution of the Belomorian belt: NORDSIM U–Pb zircon dating of the Chupa paragneisses, magmatism, and metamorphic stages. Petrology 12 (3), 195–210.

Cook, F.A., van der Velden, A.J., Hall, K.W., Roberts, B.J., 1998. Tectonic delamination and subcrustal imbrication of the Precambrian lithosphere in northwestern Canada mapped by LITHOPROBE //. Geology 26 (9), 839–842.

Cook, F.A., Clowes, R.M., Snyder, D.B., van der Velden, A.J., Hall, K.W., Erdmer, P., Evenchick, C.A., 2004. Precambrian crust beneath the Mesozoic northern Canadian Cordillera discovered by lithoprobe seismic reflection profiling //. Tectonics 23, 1–28.

De Wit, M., Tinker, J., 2004. Crustal structures across the central Kaapvaal craton from deep-seismic reflection data //. S. Afr. J. Geol. 107, 185–206.

Dokukina, K., Konilov, A., Mints, M., 2006. From eclogites to granulites: transformation of gabbroic dykes from the Gridino tectonic zone (Belomorian eclogite province, Western Fennoscandian Shield). Granulites and Granulites. Program and Abstracts, Brasiilliia, Jully 10–12, 2006, vol. 26.

Downes, H., Peltonen, P., Mänttäri, I., Sharkov, E.V., 2002. Proterozoic zircon ages from lower crustal granulite xenoliths, Kola Peninsula, Russia: evidence for crustal growth and reworking. J. Geol. Soc. 159, 485–488.

Dyadyura, V.A. (Ed.), 1992. New Methods, Processing Systems, and Interpretation of Seismic Information with Computers. Proceedings of Workshop of Association of Designers and Users of Computer-Aided Technologies for the Integrated Processing and Interpretation of Geological and Geophysical Data, Tyumen', October 7–12, 1991, Geoinformmark, Moscow, p. 145 (in Russian).

Eaton, D.W., Hynes, A., 2000. The 3-D crustal structure in the Manicouagan region: new seismic and gravity constraints //. Can. J. Earth Sci. 37, 307–324.

Eaton, D.W., Ross, G.M., Cook, F.A., Van der Velden, A., 2000. Seismic imaging of the upper mantle beneath the Rocky Mountain foreland, southwestern Alberta //. Can. J. Earth Sci. 37, 1493–1507.

Evins, P.M., Mansfeld, J., Laajoki, K., 2002. Geology and geochronology of the Suomujärvi Complex: a new Archaean gneiss region in the NE Baltic Shield, Finland. Precambrian Res. 116, 285–306.

Fountain, D.M., Boundy, T.M., Austrheim, H., Rey, P., 1994. Eclogite-facied shear zones — deep crustal reflectors? Tectonophysics 232, 411–424.

Glebovitsky, V.A. (Ed.), 2005. Early Precambrian of the Baltic Shield. Nauka, St. Petersburg (in Russian).

Hanski, E., Huhma, H., Vaasjoki, M., 2001. Geochronology of northern Finland: a summary and discussion. In: Vaasjoki, M. (Ed.), Radiometric Age Determinations from Finnish Lapland and Their Bearing on the Timing of Precambrian Volcano-sedimentary Sequences. Geological Survey of Finland, Special Paper, vol. 33, pp. 255–279.

Jackson, H.R., 2002. Seismic refraction profiles in the Gulf of Saint Lawrence and implications for extent of continuous Grenville lower crust //. Can. J. Earth Sci. 39, 1–17.

Ji, S., Long, C., Martignole, J., Salisbury, M., 1997. Seismic reflectivity of a finely layerd granulite-facies ductile shear zone in the southern Grenville Province (Quebec). Tectonophysics 279, 113–133.

Kempton, P.D., Downes, H., Neymark, L.A., Wartho, J.A., Zartman, R.E., Sharkov, E.V., 2001. Garnet granulite xenoliths from the northern Baltic Shield — the underplated lower crust of a Palaeoproterozoic large igneous province? J. Petrol. 42 (4), 731–763.

Koistinen, T., Stephens, M.B., Bogatchev, V., Nordgulen, I., Wennerström, Korhonen, J. and working group, 2001. Geological map of the Fennoscandian Shield. Scale 1: 2 000 000 Geological Surveys of Finland, Norway and Sweden and the North-West Department of Natural Resources of Russia.

Konilov, A.N., Shchipansky, A.A., Mints, M.V., 2005. Archaean eclogites from the central part of the Belomorian mobile belt, Kola Peninsula, Russia. 7th International Eclogite Conference. July 3–9, 2005, Seggau, Austria. Mitteilungen der Österreichischen Mineralogischen Gesellschaft, vol. 70.

Kontinen, A., Paavola, J., 2006. A preliminary model of the crustal structure of the eastern Finland Archaean complex between Vartius and Vieremä, based on constraints from surface geology and Fire 1 seismic survey. In: Kukkonen, I.T., Lahtinen, R. (Eds.), Finnish reflection experiment FIRE 2001–2005. Geological Survey of Finland, Special paper, vol. 43, pp. 223–240.

Korja, A., Heikkinen, P., 2005. The accretionary Svecofennian orogen — insight from the BABEL profiles. Precambrian Res. 136, 241–268.

Korja, A., Lahtinen, R., Heikkinen, P., Kukkonen, I.T., FIRE working Group, 2006. A geological interpretation of the upper crust along FIRE 1. In: Kukkonen, I.T., Lahtinen, R. (Eds.), Finnish Reflection Experiment FIRE 2001–2005. Geological Survey of Finland, Special paper, vol. 43, pp. 45–76.

Korsman, K., Korja, T., Papunen, M., Virransalo, P., GGT/SVEKA Working Group, 1999. The GGT/SVEKA Transect: structure and evolution of the continental crust in the Paleoproterozoic Svecofennian orogen in Finland. Int. Geol. Rev. 41, 287–333.

Kukkonen, I.T., Lahtinen, R., 2006. Finnish reflection experiment FIRE 2001–2005. Geological Survey of Finland, Special Paper, 43, p. 247.

Levchenkov, O.A., Nikolaev, A.A., Bogomolov, E.S., Yakovleva, S.Z., 1994. U–Pb age of the felsic Sumian volcanics in Northern Karelia. Stratigr. Geol. Correl. 2 (1), 3–9 (in Russian).

Ludden, J., Hynes, A., 2000. The Lithoprobe Abitibi–Grenville transect: two billion years of crust formation and recycling in the Precambrian Shield of Canada //. Can. J. Earth Sci. 37, 459–476.

Markwick, A.J.W., Downes, H., 2000. Lower crustal granulite xenoliths from the Arkhangelsk kimberlite pipes: petrologocal, geochemical and geophysical results. Lithos 51, 135–151.

Miller, Yu.V., 2002. Tectonics of the junction between the Belomorian mobile belt and the Karelian craton. Geotectonics 4, 14–25.

Miller, Yu.V., Baikova, N.A., Arestova, N.A., Shuleshko, I.K., 2005. A ro;e of the Khetolambina terrain in the making and early history of development of the Belomorian mobile belt. Geotectonics 2, 17–32 (in Russian).

Mints, M.V., Stupak, V.M., 2001. Methodical approaches to geological interpretation of the seismic data characterizing deep structure of the crystalline crust along the 4B profile. In: Sharov, N.V. (Ed.), Deep Structure and Evolution of the Earth's Crust in the Eastern Fennoscandian Shield: Kem–Kalevala Profile. Karelian Sci. Center, Russian Academy of Sciences, Petrozavodsk, pp. 144–156 (in Russian).

Mints, M.V., Berzin, R.G., Suleimanov, A.K., Zamozhnyaya, N.G., Stupak, V.M., Konilov, A.N., Zlobin, V.L., Kaulina, T.V., 2004a. The deep structure of the Early Precambrian crust of the Karelia craton, southeastern Fennoscandian Shield: results of investigation along CMP profile 4B. Geotectonics 38 (2), 10–29.

Mints, M.V., Berzin, R.G., Andryushchenko, Yu.N., Zamozhnyaya, N.G., Zlobin, V.L., Konilov, A.N., Stupak, V.M., Suleimanov, A.K., 2004b. The deep structure of the Karelia craton along geotraverse 1-EU. Geotectonics 38 (5), 10–25.

Mints, M.V., Kaulina, T.V., Konilov, A.N., Krotov, A.V., Stupak, V.M., 2007. The thermal and geodynamic evolution of the Lapland granulite belt: implications for thermal structure of the lower crust during granulite-facies metamorphism. Gondwana Res. 12 (3), 252–267.

Moore, V.M., Wiltschko, D.V., 2004. Syncollisional delamination and tectonic wedge development in convergent orogens. Tectonics 23, TC2005. doi:10.1029/2002TC001430.

Neymark, L.A., Nemchin, A.A., Vetrin, V.R., Salnikova, E.V., 1993. Sm–Nd and Pb–Pb isotope systematics in deep crustal xenoliths and explosive pipes of the southern part of the Kola Peninsula. Dokl. Akad. Nauk. 326 (6), 781–784 (in Russian).

Öhlander, B., Skiöld, T., Elming, S.Å., BABEL Working Group, Claesson, S., Nisca, D.H., 1993. Delineation and character of the Archean–Proterozoic Boundary in northern Sweden. Precambrian Res. 64, 67–84.

Rudnick, R.L., Fountain, D.M., 1995. Nature and composition of the continental crust: a lower crustal perspective. Rev. Geophys 33, 267–309.

Sharov N.V. (Ed.), 1997. Seismo-geological Model of the Lithosphere of Northern Europe: Lapland-Pechenga Region. Kola Sci. Center, Russian Academy of Sciences, Apatity, 225 p. (in Russian).

Sharov N.V. (Ed.), 2004. Deep Structure and Seismicity of the Karelian Region and its Surroundings. Karelian Science Centre, Russian Academy of Sciences, Petrozavodsk, 353 p. (in Russian).

Shchipansky, A., Konilov, A., Mints, M., Belousova, E., Natapov, L., Griffin, W., 2006. The Archean Salma Eclogites, Kola Peninsula, Russia: Petrology, Geochronology and Significance for Insight into the Archean Crust-forming Processes. Abstr. EGU06-A-00793.

Shchiptsov, V.V. (Ed.), 2005. Belomorian mobile belt and its analogs: geology, geochronology, geodynamics and metallogeny. Proceedings of the Scientific Conference and Field Trip Guide Book. Karelian Sci. Center, Russian Academy of Sciences, Petrozavodsk, p. 333 (in Russian).

Slabunov, A.I., 2005. Geology and Geodynamics of the Belomorian Mobile Belt of the Fennoscandian Shield. Doctoral Dissertation in Geology and Mineralogy. Moscow, 2005.

Slabunov, A.I., Lobach-Zhuchenko, S.B., Bibikova, E.V., Sorjonen-Ward, P., Balagansky, V.V., Volodichev, O.I., Shchipansky, A.A., Svetov, S.A., Chekulaev, V.P., Arestova, N.A., Stepanov, V.S., 2006. The Archaean nucleus of the Fennoscandian (Baltic) Shield. In: Gee, D.G., Stephenson, R. (Eds.), European Lithosphere Dynamics. Geological Society, London, Memoirs, vol. 32, pp. 627–644.

Sokolov, V.A. (Ed.), 1987. Geology of Karelia. Nauka, Leningrad, p. 231 (in Russian).

Stupak, V.M., 2000. Differential seismic survey as a tool for detailed studies of geological sections. Untraditional Methods of Mineral Resources Exploration. Collection of the Scientific Works of the Northwestern Department of Natural Resources. St. Petersburg, pp. 164–176 (in Russian).

Tugarinov, A.I., Bibikova, E.V., 1980. Geochronology of the Baltic Shield from Zircon Data. Nauka, Moscow. 131 p.

Vasil'ev, S.A., Urupov, A.K., 1978. New possibilities to study of seismic wave velocities and medium structure from observations in reciprocal points. Applied Geophysics. Nedra, Moscow, No 92, pp. 3–16 (in Russian).

Vetrin, V.R., 2006. A composition and structure of the lower crust of the Belomorian mobile belt, Baltic Shield. Petrology 14 (4), 415–438.

Volodichev, O.I., Slabunov, A.I., Bibikova, E.V., Konilov, A.N., Kuzenko, T.I., 2004. The Archaean eclogites of the Belomorian mobile belt, Baltic Shield. Petrology 12 (6), 540–560.

Zlobin, V.L., Bogina, M.M., Mints, M.V., 2005. Felsic Palaeoproterozoic metavolcanics of the Lehta structure. Proceedings of the X All-Russia Petrography Conference. Geol. Inst. of the Kola Sci. Centre, Apatity, vol. 3, pp. 120–122 (in Russian).